Proceedings of the ICBBG2025
2025 International conference on Bio-mediated and Bio-inspired Geotechnics
18-20 May, 2025 | Tempe, Arizona, USA
https://doi.org/10.53243/ICBBG2025-100

Interface Shear Directionality Between Snakeskin-Inspired Surfaces and Normally Consolidated and Compacted Fine-Grained Soils

Hyeon Jung Kim[1] and Alejandro Martinez[2]

[1]Department of Civil and Environmental Engineering, University of California Davis, 2001 Ghausi Hall, Davis CA, 95616; e-mail: hyki@ucdavis.edu
[2]Department of Civil and Environmental Engineering, University of California Davis, 2001 Ghausi Hall, Davis CA, 95616; e-mail: amart@ucdavis.edu

ABSTRACT

The ventral scales of snakes mobilize direction-dependent friction, generating higher interface strength in the cranial direction (i.e., against the asperities) compared to the caudal one (i.e., along the asperities). This direction-dependence holds potential for enhancing the performance of geotechnical applications such as foundations, anchors, and soil reinforcement elements. This study evaluates the shear behavior of snakeskin-inspired surfaces in contact with normally consolidated kaolin clay and compacted silty clay through interface shear tests. The test results are used to evaluate the effect of asperity geometry and shearing direction on the interface shear behavior with two distinct fine-grained soils. For both soils, shearing in the cranial direction resulted in greater peak and residual strengths than shearing in the caudal one. The compacted silty clay exhibited higher shear resistances than the normally consolidated clay, with a more pronounced difference between the cranial and caudal interface shear strengths. The strength with both soils increases as the asperity height is increased and the length is decreased. The findings highlight the potential to leverage the directional-dependent strength of snakeskin-inspired surfaces to enhance the capacity and multifunctionality of various geotechnical applications.

INTRODUCTION

Foundation elements such as piles and soil anchors can be subjected to axial loads in both tension and compression, presenting a design challenge due to the opposing demands of installation and pullout performance. High skin friction enhances tensile capacity but increases installation forces, while low friction is beneficial for installation but compromises capacity. To address these conflicting requirements, there is a growing interest in surfaces with direction-dependent skin friction. Such surfaces can reduce installation forces while increasing pullout capacity. A thorough understanding of load transfer mechanisms, influenced by factors like soil type, drainage conditions, and surface geometry, is essential for developing effective design methods that incorporate direction-dependent skin friction.

Soil-structure interfaces play a critical role in the stability and performance of geotechnical structures such as foundations, anchors, and reinforced retaining walls. Extensive research over the past few decades has elucidated the factors influencing interface behavior in sand and clay. For sand, studies have shown that interface strength is governed by factors such as surface roughness, particle angularity, and soil density (Uesugi and Kishida, 1986; Dove and Frost 1999; DeJong and Westgate 2009; Martinez and Frost, 2017). The surface roughness is a key factor

controlling the interface strength in clays, with rougher surfaces leading to greater strength. The OCR has been shown to impact the interface strength, with higher OCR values leading to increased strength (Subba Rao et al., 2000; Martinez and Stutz, 2019). Shearing velocity also plays a significant role, affecting the drainage conditions and, consequently, the interface shear strength (Lemos and Vaughan, 2000; Boukpeti and White, 2017; Martinez and Stutz, 2019). Understanding these factors is crucial for optimizing the design and performance of soil-structure interfaces in various geotechnical applications.

Animals and plants interact with soils in ways similar to engineered structures, involving processes like soil penetration, excavation, and load transfer (Martinez et al., 2022). Bio-inspired designs have recently been applied in geotechnical engineering, particularly in deep foundations, soil anchors, and site characterization (Martinez et al., 2022; Martinez et al., 2024a). Among these organisms, snakes use their ventral scales to generate lower frictional forces when moving forward (i.e., in the caudal direction) compared to when moving backward (i.e., in the cranial direction) (Marvi and Hu, 2012; Marvi et al., 2014). Recent studies on snakeskin-inspired surfaces have primarily focused on sand, demonstrating that higher strengths are mobilized in the cranial direction due to the increased interlocking and mobilization of passive resistances (Martinez et al., 2019; Xiao et al., 2023; Lee et al., 2023). Laboratory experiments have shown that increasing the asperity height and decreasing the asperity length increase interface strength, regardless of sand particle size, density, or mineralogy (Martinez et al., 2019; Nawaz et al., 2024; Stutz and Martinez 2021; Xiao et al., 2023). Furthermore, centrifuge tests on snakeskin-inspired piles and field tests of anchors have shown greater shaft resistance during cranial pullout in sandy and silty soils (O'Hara and Martinez 2022; Martinez et al. 2024b).

This study investigates the shear behavior of snakeskin-inspired surfaces in contact with normally consolidated kaolin clay and compacted silty clay. The research aims to evaluate the influence of asperity geometry and shearing direction on the interface load transfer behavior with two distinct types of fine-grained soils. The results highlight the potential of these snakeskin-inspired surfaces to enhance the capacity and performance of various geotechnical systems through directional-dependent load transfer.

METHODS

Direct interface shear tests were performed on normally consolidated (NC) kaolin clay and compacted silty clay specimens. These specimens were tested in a shear box with dimensions of 100.0 mm in length and 63.5 mm in width. Figure 1a shows a schematic of the interface shear box device configuration. This study considered two reference surfaces. Specifically, the smooth surface is made of polished steel and has a maximum surface roughness (R_{max}) of 12.8 μm and an average surface roughness (R_a) of 3.1 μm. The rough surface is composed of steel coated with epoxied Ottawa 20-30 sand and has R_{max} and R_a values of 1098.4 μm and 157.7 μm, respectively.

The bio-inspired surfaces were fabricated from photosensitive resin using a Form 3 printer, following the procedures outlined by Martinez and Palumbo (2018) and Martinez et al. (2019). The 3D printing process employed a layer thickness of 0.05 mm, which is much smaller than the differences in asperity height and length between the different snakeskin-inspired surfaces. These surfaces have asperities inspired by the ventral scales of the western hognose snake, which were simplified into straight-lined, triangular shapes as shown in Figure 1b. The snakeskin-inspired surfaces have asperity heights (H) ranging from 0.1 to 0.8 mm and lengths (L) varied from 6 to 24 mm (Table 1). Figure 1c shows photographs of three of these snakeskin-inspired surfaces. The

surfaces were labeled using the "*AA HBBLCC* " convention, where "*AA*" indicates the shearing direction, with "*CR*" for cranial and "*CD*" for caudal shearing, "*BB*" denotes the asperity height in mm, and "*CC*" specifies the asperity length in mm. Previous studies by Martinez et al. (2019) and Martinez et al. (2024b) demonstrated that snakeskin-inspired surfaces can also be effectively characterized by the *L/H* ratio, which in the current study is varied between 15 and 120 (Table 1).

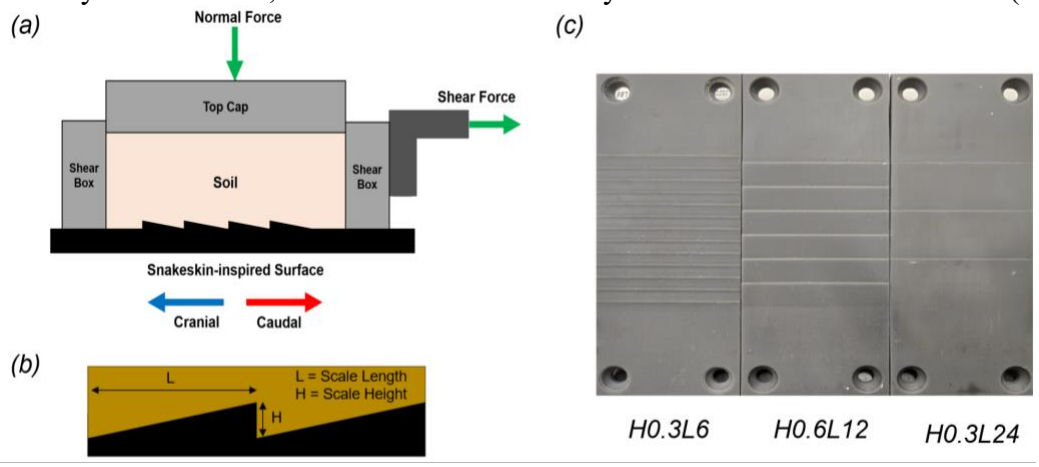

Fig. 1. Schematic of (a) interface shear testing configuration, (b) geometrical asperity characteristics of asperities, and (c) snakeskin-inspired surfaces used for laboratory testing.

Table 1. Geometrical characteristics of snakeskin-inspired surfaces.

Surface	Scale Length, *L* (mm)	Scale Height, *H* (mm)	Scale Geometry Ratio, *L/H*	Average Roughness, R_a (μm)	Maximum Roughness, R_{max} (μm)
H0.8L12	12	0.8	15	191.8	738.7
H0.6L12	12	0.6	20	137.0	528.1
H0.3L6	6	0.3	20	73.1	339.8
H0.3L12	12	0.3	40	71.4	267.7
H0.3L18	18	0.3	60	68.4	266.8
H0.3L24	24	0.3	80	74.6	299.0
H0.1L12	12	0.1	120	37.0	124.8
Smooth	--	--	--	3.1	12.8
Rough	--	--	--	157.7	1098.4

Normally Consolidated Kaolin Clay.

Interface shear tests were performed on specimens of kaolin clay that had a liquid limit (L_L) of 50.1%, plastic limit (P_L) of 22.4%, compression index (C_C) of 0.29, recompression index (C_r) of 0.07, specific gravity (G_S) of 2.67, and coefficient of consolidation (C_v) of 0.105 mm²/s at an effective vertical stress of 80 kPa (Table 2). The specimens for interface shear testing were prepared by thoroughly mixing dry powdered clay with deionized water to achieve a water content corresponding to 1.2 times L_L, following the method outlined in Martinez and Stutz (2019). All specimens were then consolidated to an effective stress of 75 kPa. The tests presented here were conducted at a rate of 4 mm/min, which was sufficiently large to induce undrained conditions in tests with a similar kaolin clay (Martinez and Stutz, 2019). Results of preliminary tests against the rough surface show that both peak and residual shear strengths decrease with increasing shearing

velocity due to the generation of positive excess pore pressures. Shearing velocities equal or greater than 1 mm/min resulted in similar strengths, indicating the presence of undrained conditions at these rates.

Compacted Silty Clay.

Interface shear tests were performed on specimens of silty clay known locally as Yolo loam. The soil has a L_L of 33.5%, P_L of 17.7%, G_S of 2.65, fines fraction of 58%, maximum dry unit weight of 17.3 kN/m^3, and an optimum moisture content of 14.5% determined following ASTM D698-12 standards (ASTM 2012) (Table 2). The interface shear tests were performed on compacted specimens with a target relative density of 95% (dry unit weight of 16.4 kN/m^3) and water content of 10.5%, resulting in a void ratio of 0.58 and a degree of saturation of 48%. The specimens were compacted by tamping in five layers to achieve the desired dry unit weight. Tests were performed at normal stresses (σ_{n0}) of 75 kPa. All tests were conducted at a shear rate of 1 mm/min under constant normal load (CNL) boundary conditions. Based on the applied shearing rate and the unsaturated state of the specimens, the drainage conditions are expected to be either partially-drained or drained during all the tests.

Table 2. Properties of tested soils.

Property	Kaolin Clay	Yolo Loam
Soil classification (USCS)	CH	CL
Liquid limit (%)	50.1	33.5
Plastic limit (%)	22.4	17.7
Particle specific gravity	2.67	2.65
Compression index, C_C	0.29	-
Swelling index, C_S	0.07	-
Coefficient of consolidation, c_v (mm^2/s)*	0.11	-
Fines fraction (%)	-	57.7
Maximum dry unit weight (kN/m^3)#	-	17.3
Optimum water content (%)#	-	14.5

*OCR = 1, σ'_v = 80 kPa, #Standard Proctor test

RESULTS

Normally Consolidated Kaolin Clay.

The results of monotonic interface shear tests on the five snakeskin-inspired surfaces on NC clay are presented in terms of shear stress-displacement curves for cranial and caudal tests. Figure 2 shows the results of tests against the rough, smooth, and snakeskin-inspired surfaces. As anticipated, the rough surface mobilized higher shear stresses and induced greater vertical displacements than the smooth surface due to the more substantial soil deformations (Figure 2a and 2b) (Martinez and Stutz 2019). The snakeskin-inspired surfaces exhibited higher shear strengths in the cranial direction than in the caudal direction across all H and L values, although the vertical displacements were similar in both directions (Figure 2a-f). Increases in H and decreases in L led to higher peak and residual interface shear strengths. For a constant H of 0.3 mm, initial increases in L resulted in sharper decreases in peak and residual strengths (Figure 3a and 3b). Conversely, with a constant L of 12 mm, initial increases in H resulted in greater increases in strengths (Figure 3c and 3d).

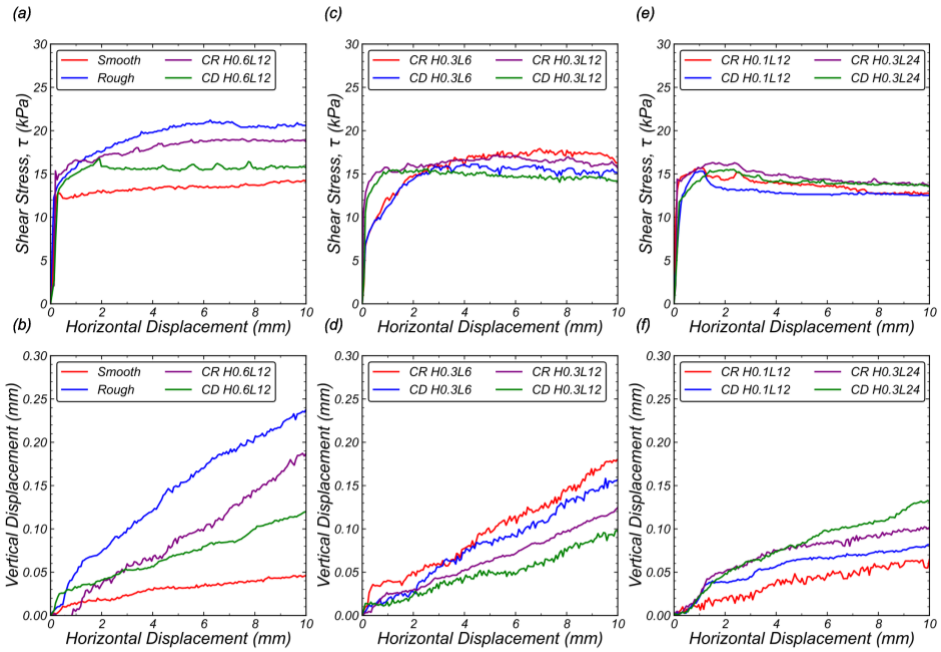

Fig. 2. Results of interface shear tests on NC clay specimens against: (a-b) with smooth, rough, and H0.6L12, (c-d) H0.3L6 and H0.6L12, and (e-f) H0.1L12 and H0.3L24 surfaces.

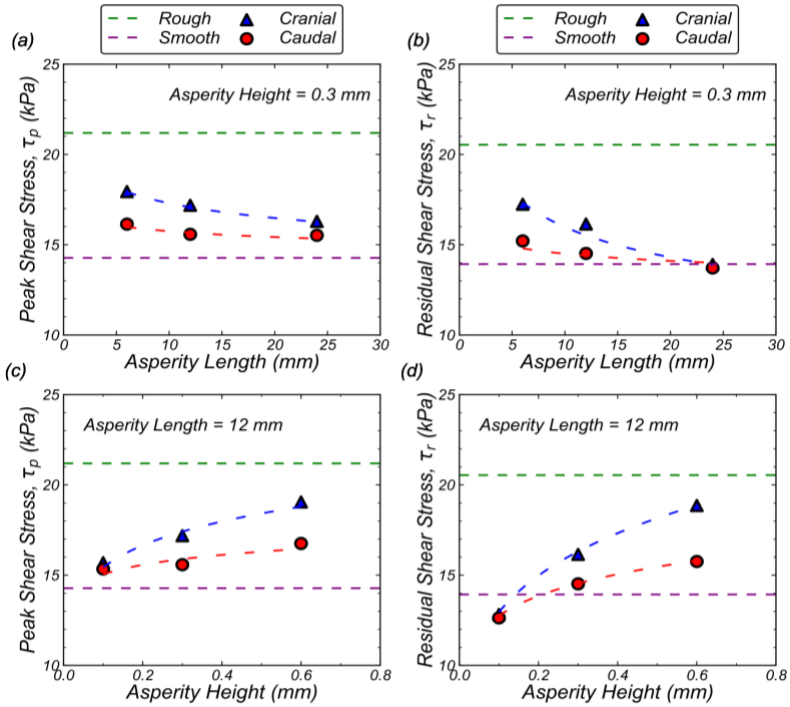

Fig. 3. Peak and residual strength of NC clay as a function of: (a-b) *L* for a constant *H* of 0.3 mm, and (c-d) *H* for a constant *L* of 12 mm.

Compacted Silty Clay.

The interface shear tests on the compacted silty clay highlight the significant influence of the surface characteristics on the shear strength and vertical displacements in unsaturated conditions. Figure 4 indicates that the rough surface mobilized high shear stresses and exhibited a dilative response, whereas the smooth surface generated the lowest peak shear strength and negligible vertical displacements. Similar to the results with NC clay with snakeskin-inspired surfaces, cranial shearing generated greater strengths than caudal shearing (Figure 4), and increases in H and decreases in L led to higher peak and residual interface shear strengths (Figure 5). However, the bio-inspired surfaces exhibited higher peak and residual shear stress in the cranial direction for high H and low L than the rough surface (Figures 5b and 5d).

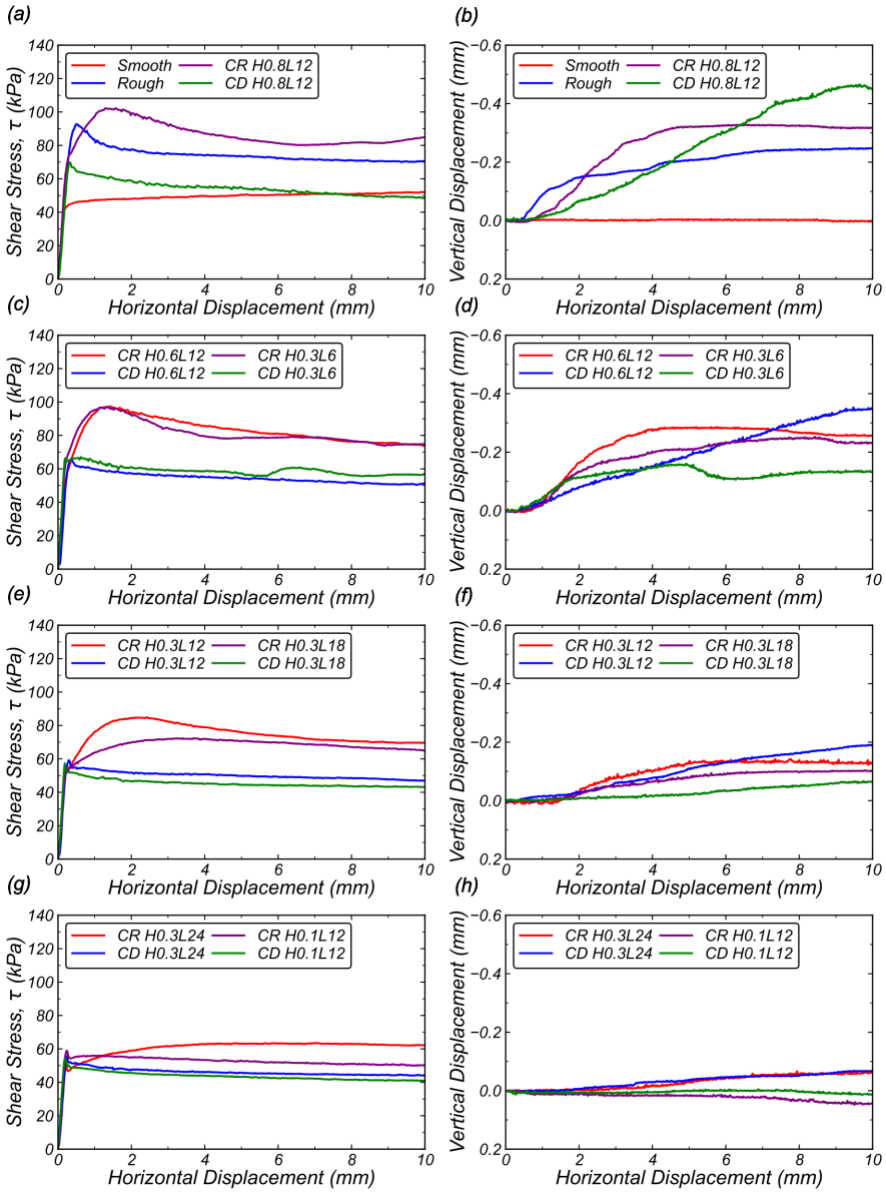

Fig. 4. Results of interface shear tests on compacted silty clay specimens against: (a-b) smooth, rough, and H0.8L12, (c-d) H0.6L12 and H0.3L6, (e-f) H0.3L12 and H0.3L18, and (g-h) H0.3L24 and H0.1L12 surfaces.

Repeatability.

Several of the interface shear tests were conducted two times to verify the repeatability of the results. For the tests performed under undrained conditions with kaolin clay, the variability obtained based on 9 pairs of identical tests yielded minimum, average, and maximum errors in the mobilized shear strength of 2.8%, 8.3%, and 13.7%, respectively. Similarly, for the compacted silty clay, 10 pairs of identical tests yielded minimum, average, and maximum errors in the mobilized shear strength of 1.0%, 3.9%, and 7.7%, respectively. These differences are significantly smaller than those due to differences in asperity height and length, as shown in the following section. Therefore, the experimental variability is deemed to be appropriate and is not discussed in the analysis presented below.

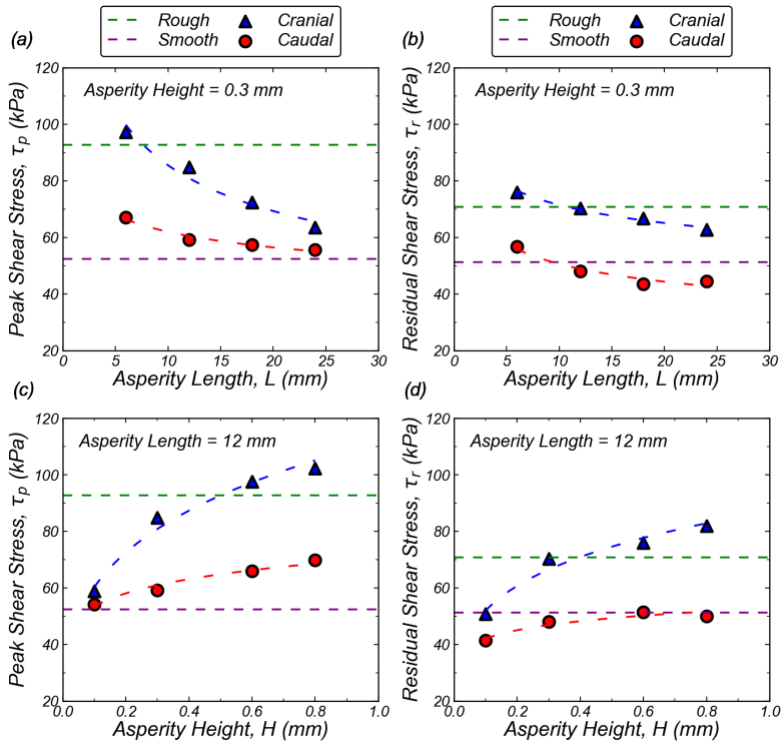

Fig. 5. Peak and residual strength of compacted silty clay as a function of: (a-b) *L* for a constant *H* of 0.3 mm, and (c-d) *H* for a constant *L* of 12 mm.

Effect of asperity geometry on interface shear strength.

The influence of the asperity geometry on the interface strength was systematically examined for both the NC clay and compacted silty clay. Figure 6 illustrates the effect of the ratio of asperity length to height on the interface response. As shown, the *L/H* parameter unifies the data in specific relationships for each soil type. A decrease in *L/H*, achieved through either a reduction in *L* or an increase in *H*, results in higher peak and residual stresses, as well as a greater difference between the cranial and caudal strengths. The variations in cranial and caudal peak and residual shear strength ratios are more pronounced in the compacted silty clay than in the NC clay, especially at lower *L* and higher *H* values. For instance, the peak shear stress ratios for NC clay on snakeskin-inspired surfaces range from 0.20 to 0.25, whereas those for compacted silty clay range from 0.72 to 1.36.

To quantify the relative differences in shear resistances mobilized in the cranial and caudal

directions, the ratio of the cranial to caudal interface shear strength as a function of the *L/H* ratio is shown in Figure 7. The NC clay exhibits lower values, indicating smaller differences in cranial and caudal strength compared to the compacted silty clay. Specifically, for both peak and residual shear strengths, the snakeskin-inspired surfaces mobilized strengths in the cranial direction that were between 1.01 and 1.20 times greater than those in the caudal direction (Figure 7a and b). In comparison, for compacted silty clay, the peak and residual shearing values in the cranial direction were between 1.09 and 1.64 times greater than the corresponding values in the caudal direction (Figure 7c and d). These findings indicate that the compacted silty clay is more significantly affected by asperity geometry in terms of interface shear strength and strength directionality than the NC clay.

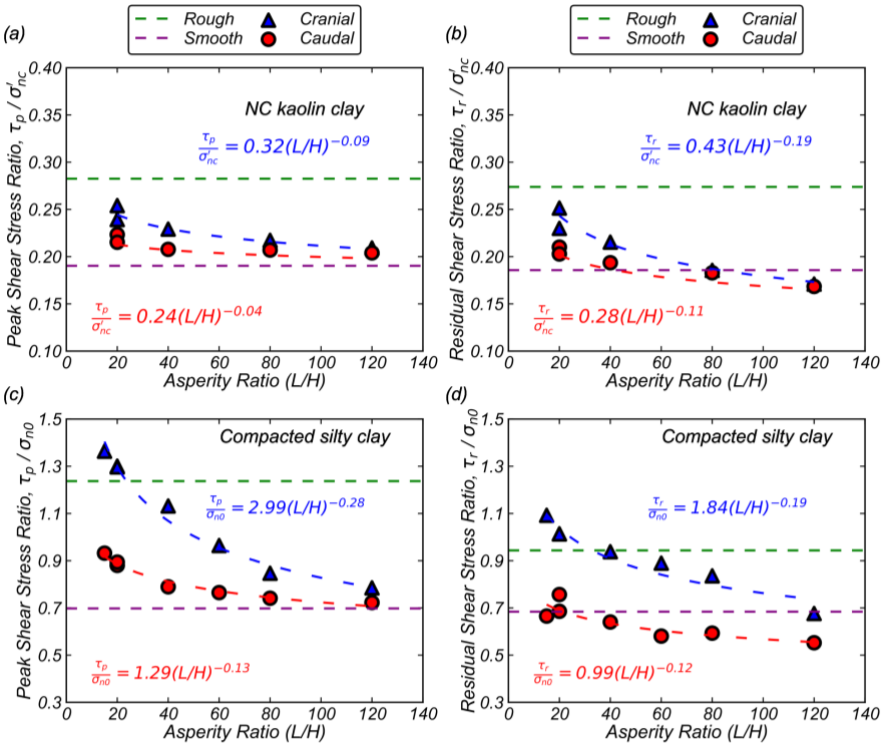

Fig. 6. Peak and residual shear stress ratio of tests at normal effective stress of 75 kPa on (a-b) NC clay and (c-d) compacted silty clay specimens as a function of *L/H*. Note that different y-axis ranges are used in (a-b) and (c-d).

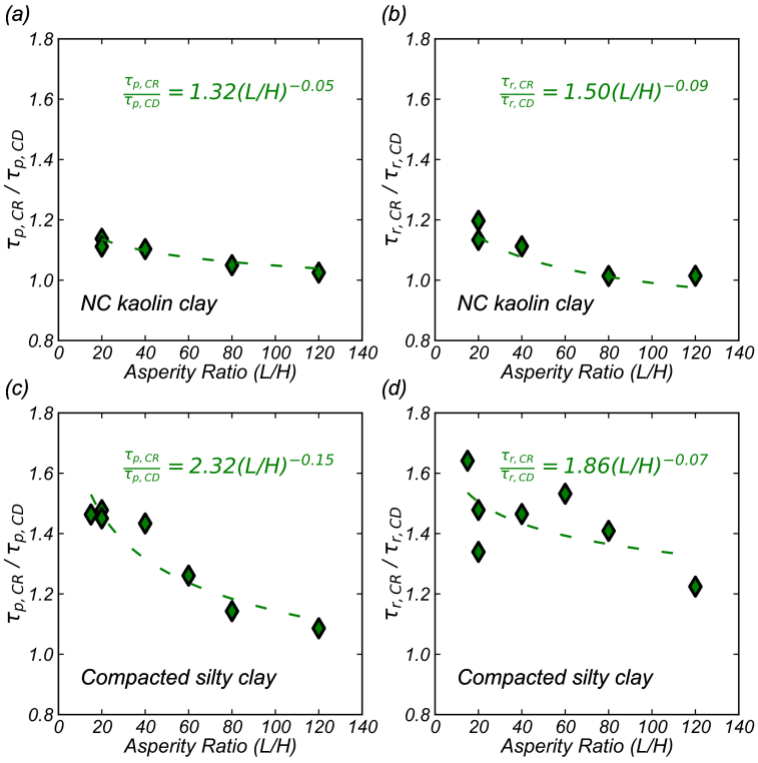

Fig. 7. Ratio of cranial to caudal interface shear strength at normal effective stress of 75 kPa for (a-b) NC clay and (c-d) compacted silty clay as a function of *L/H*.

CONCLUSION

This study demonstrates that interfaces between snakeskin-inspired surfaces and fine-grained soils exhibit direction-dependent shear strength. Cranial shearing consistently mobilized greater shear strengths than caudal shearing, with the effect being more pronounced in the compacted silty clay compared to the normally consolidated clay. Increasing asperity height and decreasing asperity length increased both peak and residual shear strengths, with the ratio of asperity length to height (i.e., *L/H*) effectively characterizing these variations. Differences in asperity geometry resulted in greater differences in strength on the compacted silty clay than on the NC clay. In addition, the compacted silty clay yielded greater differences between cranial and caudal strength. The interface strength mobilized by the snakeskin-inspired surfaces with the NC clay was smaller than that mobilized by the rough surface. In contrast, the strength with snakeskin-inspired surfaces with high asperity heights and small lengths mobilized greater strengths than the rough surface for the compacted silty clay. The micro-mechanisms underlying the interaction between soil particles and surface asperities should be further investigated to understand the effects of particle interlocking, asperity deformation, and stress distribution. These results indicate that cranial shearing generates greater shear strength than caudal shearing in a range of fine-grained soil types and asperity geometries. This directionality in strength can facilitate reduction in installation loads while simultaneously increasing pullout resistances. The fact that the *L/H* ratio uniquely captures the effect of asperity geometry can help in design in situations where producing small asperities is impractical, for example for deep foundations. In these cases, both L and H can be upscales proportionally, and the relationship with *L/H* determined from laboratory tests can be used to estimate the interface strength. Overall, the results presented here suggest that the snakeskin-inspired surfaces can be leveraged to improve the multifunctionality, efficiency and reliability of

foundations, anchors, and soil reinforcement elements in fine-grained soils.

ACKNOWLEDGEMENT

This material is based on work supported by the Engineering Research Center Program of the National Science Foundation under NSF Cooperative Agreement No. EEC-1449501. Any opinions, findings, and conclusions expressed in this material are those of the author(s) and do not necessarily reflect those of the NSF.

REFERENCES

ASTM. 2012. *Standard test method for laboratory compaction characteristics of soil using standard effort*. ASTM D698. West Conshohocken, PA : ASTM.

Boukpeti, N., & White, D. J. (2017). Interface shear box tests for assessing axial pipe–soil resistance. *Géotechnique*, *67*(1), 18–30. https://doi.org/10.1680/jgeot.15.p.112

DeJong, J. T., & Westgate, Z. J. (2009). Role of initial state, material properties, and confinement condition on local and global soil-structure interface behavior. *Journal of Geotechnical and Geoenvironmental Engineering*, *135*(11), 1646–1660. https://doi.org/10.1061/(asce)1090-0241(2009)135:11(1646)

Dove, J. E., & Frost, J. D. (1999). Peak friction behavior of smooth geomembrane-particle interfaces. *Journal of Geotechnical and Geoenvironmental Engineering*, *125*(7), 544–555. https://doi.org/10.1061/(asce)1090-0241(1999)125:7(544)

Lee, S.-H., Nawaz, M. N., & Chong, S.-H. (2023). Estimation of interface frictional anisotropy between sand and snakeskin-inspired surfaces. *Scientific Reports, 13*(1). https://doi.org/10.1038/s41598-023-31047-3

Lemos, L. J., & Vaughan, P. R. (2000). Clay–interface shear resistance. *Géotechnique*, *50*(1), 55–64. https://doi.org/10.1680/geot.2000.50.1.55

Martinez, A., & Frost, J. D. (2017). The influence of surface roughness form on the strength of sand–structure interfaces. *Géotechnique Letters*, *7*(1), 104–111. https://doi.org/10.1680/jgele.16.00169

Martinez, A., Chen, Y., & Anilkumar, R. (2024a). Bio-inspired site characterization - towards soundings with lightweight equipment. *7th International Conference on Geotechnical and Geophysical Site Characterization*. https://doi.org/10.23967/isc.2024.316

Martinez, A., & Palumbo, S. (2018). Anisotropic shear behavior of soil-structure interfaces: Bio-inspiration from Snake Skin. *IFCEE 2018*. https://doi.org/10.1061/9780784481592.010

Martinez, A., & Palumbo, S., & Todd, B. D. (2019). Bioinspiration for anisotropic load transfer at soil–structure interfaces. *Journal of Geotechnical and Geoenvironmental Engineering*, *145*(10). https://doi.org/10.1061/(asce)gt.1943-5606.0002138

Martinez, A., & Stutz, H. H. (2019). Rate effects on the interface shear behaviour of normally and overconsolidated clay. *Géotechnique*, *69*(9), 801–815. https://doi.org/10.1680/jgeot.17.p.311

Martinez, A., DeJong, J.,et al. (2022). Bio-inspired geotechnical engineering: Principles, current work, opportunities and challenges. *Géotechnique*, *72*(8), 687–705. https://doi.org/10.1680/jgeot.20.P.170

Martinez, A., & Zamora, F., & Wilson, D. (2024b). Field evaluation of the installation and pullout of snakeskin-inspired anchorage elements. *Journal of Geotechnical and Geoenvironmental Engineering*, *150*(8). https://doi.org/10.1061/jggefk.gteng-12311

Marvi, H., & Hu, D. L. (2012). Friction enhancement in concertina locomotion of snakes. *Journal of The Royal Society Interface*, *9*(76), 3067–3080. https://doi.org/10.1098/rsif.2012.0132

Marvi, H., Gong, C., Gravish, N., Astley, H., Travers, M., Hatton, R. L., Mendelson, J. R., Choset, H., Hu, D. L., & Goldman, D. I. (2014). Sidewinding with minimal slip: Snake and robot ascent of Sandy Slopes. *Science*, *346*(6206), 224–229. https://doi.org/10.1126/science.1255718

Nawaz, M. N., Lee, S.-H., Chong, S.-H., & Ku, T. (2024). Interface frictional anisotropy of dilative sand. *Scientific Reports*, *14*(1). https://doi.org/10.1038/s41598-024-56621-1

O'Hara, K.B. & Martinez, A. (2022). Load transfer directionality of snakeskin-inspired piles during installation and pullout in sands. *Journal of Geotechnical and Geoenvironmental Engineering*, 148(12). https://doi.org/10.1061/jggefk.gteng-12311

Stutz, H. H., & Martinez, A. (2021). Directionally dependent strength and dilatancy behavior of soil–structure interfaces. *Acta Geotechnica*, *16*(9), 2805–2820. https://doi.org/10.1007/s11440-021-01199-5

Subba Rao, K. S., Allam, M. M., & Robinson, R. G. (2000). Drained shear strength of fine-grained soil–solid surface interfaces. *Proceedings of the Institution of Civil Engineers - Geotechnical Engineering, 143(2)*, 75–81. https://doi.org/10.1680/geng.2000.143.2.75

Uesugi, M., & Kishida, H. (1986). Frictional resistance at yield between dry sand and mild steel. Soils and Foundations, 26(4), 139–149. https://doi.org/10.3208/sandf1972.26.4_139

Xiao, Y., Cui, H., Shi, J., Qiao, W., & Stuedlein, A. W. (2023). Shear response of calcareous sand-steel snake skin-inspired interfaces. *Acta Geotechnica, 19*(3), 1517–1527. https://doi.org/10.1007/s11440-023-02151-5